ORIGINAL ARTICLE

Proteasomal activity-based probes mark protein homeostasis in muscles

Vered Raz[1]*, Yotam Raz[1], Guillem Paniagua-Soriano[2], Jacomina Cornelia Roorda[1], Cyriel Olie[1], Muhammad Riaz[1] & Bogdan I. Florea[2]

[1]Department of Human Genetics, LUMC, Leiden, The Netherlands; [2]Bio-organic Synthesis, Leiden Institute of Chemistry, Leiden, The Netherlands

Abstract

Background   Protein homeostasis, primarily regulated by the ubiquitin–proteasome system is crucial for proper function of cells. In tissues of post-mitotic cells, the impaired ubiquitin–proteasome system is found in a wide range of neuromuscular disorders. Activity-based probes (ABPs) measure proteasomal proteolytic subunits and can be used to report protein homeostasis. Despite the crucial role of the proteasome in neuromuscular pathologies, ABPs were not employed in muscle cells and tissues, and measurement of proteasomal activity was carried out *in vitro* using low-throughput procedures.
Methods   We screened six ABPs for specific application in muscle cell culture using high throughput call-based imaging procedures. We then determined an *in situ* proteasomal activity in myofibers of muscle cryosections.
Results   We demonstrate that LWA300, a pan-reactive proteasomal probe, is most suitable to report proteasomal activity in muscle cells using cell-based bio-imaging. We found that proteasomal activity is two-fold and three-fold enhanced in fused muscle cell culture compared with non-fused cells. Moreover, we found that proteasomal activity can discriminate between muscles. Across muscles, a relative higher proteasomal activity was found in hybrid myofibers whereas fast-twitch myofibers displayed lower activity.
Conclusions   Our study demonstrates that proteasomal activity differ between muscles and between myofiber types. We suggest that ABPs can be used to report disease progression and treatment efficacy.

Keywords   Proteasomal activity; Activity probes; Cell-based imaging; Cellomics; Flow cytometry

Introduction

Maintenance of protein homeostasis is essential for normal cellular function. In post-mitotic cells, like muscles and neurons, protein homeostasis is predominantly regulated by autophagy and the ubiquitin–proteasome system, and in a wide range on neuromuscular pathologies, the proteasomal activity and/or autophagy are often impaired.[1–3] Although both cellular machineries are molecularly interconnected, the proteasome is the prominent machinery of protein degradation, in part because autophagy is cytoplasmic, whereas the proteasome is nuclear and cytoplasmic.[1,3] Impaired proteasomal activity fuels the accumulation of misfolded proteins and formation of protein aggregates, a pathological hallmark of many ageing-associated pathologies.[4] Proteasomal activity could be an informative measure of cellular pathology and response to drugs.

The constitutive 26S proteasome consists of a 20S catalytic core, capped at each end by a 19S regulatory particle that regulates the entry of proteins into the proteolytic cavity of the 20S core.[5] The 20S protein complex is composed of two central β-subunits rings flanked at each end by a ring of α-subunits. The catalytic core is a modular protein complex, and proteolysis is executed by the β1, β2, and β5 subunits, which possess caspase-like, trypsin-like, and chymotrypsin-like specific activities, respectively.[6] Libraries of specific proteasomal inhibitors led to the development of activity-based probes monitoring proteasomal activity (reviewed in

Carmony and Kim,[7] and Sieber[8]). The proteasome activity-based probes (ABPs) are proteasomal inhibitors conjugated to a fluorophore that irreversibly bind to the catalytic β-subunits. ABPs can bind to the β1, β2, and β5 subunits collectively or each subunit separately[7,9] (Figure 1A). Those ABPs specifically bind to the activated proteasomal subunits allowing direct, accurate quantification of the proteasome. Proteasomal activity can be measured using a number of reliable assays measuring chymotrypsin-like, trypsin-like, and caspase-like protease activities using fluorogenic substrates.[10] Their major shortcomings are as follows: low-throughput, not cell-based, not subunit-specific, and not suitable to report proteasomal activity in tissue sections.[10]

Impaired protein homeostasis is associated with degenerated muscles and muscle pathologies.[2,11] Decreased proteasome activity in human muscles is age-associated,[12] whereas in rats, proteasome activity in muscles increases with age.[13] We reported that proteasome activity is reduced in a mouse model for muscle ageing.[14] Despite the prominent role of the proteasome in maintaining protein homeostasis in muscles, the changes in proteasomal activity with age are not fully understood. In most studies, measurements of proteasomal activity in muscles and in muscle cell culture are carried out predominantly by low-throughput biochemical assays.[12,15,16] Robust and accurate measurement of proteasomal activity could report altered myogenesis and muscle function. Here, we report the application of ABPs in muscle cell culture and in muscle cryosections. We screened six ABPs and demonstrate selective application of those ABPs

in high-throughput cell-based imaging procedures (summarized in Figure 1B). Moreover, we show that the binding efficacy of ABPs can differ between myofiber types and discriminate between muscles. Our study demonstrates that proteasomal activity probes can specifically monitor proteasomal activity in skeletal muscles and open new options to investigate altered protein homeostasis in degenerated muscles and aged muscles.

Methods

Activity-based probes and inhibitors

Pan-reactive ABPs (LWA300, MV151, and MVB003) were previously described.[17–19] Subunit-specific ABPs LW124 and MVB127, targeting β1 and β5 respectively, were described in Verdoes et al.,[20] and PR592 (β5) in Geurink et al.[21] Inhibitors used in this study: Epox 1-0.5 µM (Sigma-Aldrich, MO, USA); MG132 10 µM (Sigma-Aldrich, MO, USA); IU1 50 µM (AG Scientific). The subunit-specific inhibitors, NC-001 (0.5 µM) and NC-005 (1-0.5 µM), were reported in Britton et al.[22]

Cell culture

Immortalized mouse myoblasts, C2C12, were propagated as described in de Klerk et al.[23] Immortalized human myoblasts,

Figure 1 Screen of proteasome activity-based probes in muscle cell culture. (A) Six activity probes, divided into pan-reactive and subunit-specific, were included in the study. Probes are classified between pan-reactive, which bind to all catalytic β-subunits, or subunit-specific (β1 or β5). The active subunits β1, β2, and β5 are marked by yellow, blue, and red symbols, respectively. (B) The flow chart summarizes the screening procedure for the study in muscles. All six probes were tested for binding specificity in muscle cell culture using activity gels. The probes demonstrated specific activities in muscle cells were then assayed in living cells with cell-based imaging procedures. Only LWA300 demonstrated specific binding and was assayed in muscles.
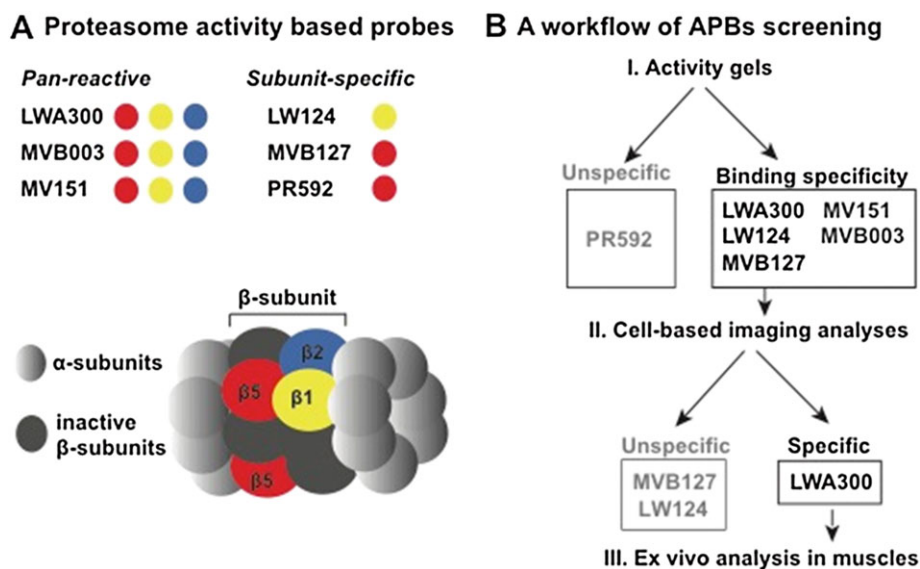
7304.1, were cultured according to Anvar *et al.*[24] shUsp14 cell line was generated by transfection of shRNA clone TRCN0000007428 (Sigma-Aldrich, MO, USA) into C2C12 using Lipofectamin 2000 (Invitrogen) according to the manufacturer manual. Scramble shRNA line was previously described.[14] Stable culture was generated by puromycin selection. Cultures were propagated in a growth medium with puromycin (2.5 μg/mL). Prior to LWA300 incubation, puromycin was removed for 2–3 cell duelling.

Molecular analysis of the shUsp14 line was carried out using RT-qPCR and Western blot analysis as described in de Klerk *et al.*[23] *Usp14* was detected using the primer set, designed by Primer 3 plus. The Usp14 protein was detected using the GTX115186 polyclonal antibody (Gene Tex, Irvine, CA, USA). The tubulin antibody was purchased from Sigma-Aldrich.

Activity-based probe analysis in activity gels

Activity-based probe binding to active proteasome subunits in C2C12 was determined using activity gels. Specific binding was determined by pre-incubation with Epox 1 μg/mL Epox (Sigma-Aldrich, MO, USA); DMSO (1:1000; Mock) for 1 h at 37°C in a growth medium, following by an incubation with the ABP (0.5 μM) for 1 h at 37°C in a growth medium. Pre-incubation with other inhibitors was also carried out for 1 h at 37°C in a growth medium. Subsequently, cells were harvested by trypsinization, and cell pellets were stored in −80°C prior to analysis. Protein lysate was carried out in a lysis buffer containing the following: 50 mM Tris-HCl [pH 7.5], 250 mM sucrose, 5 mM $MgCl_2$, 1 mM DTT, 2 mM ATP, 0.025% digitonin, 0.2% NP40. Protein aliquots were resolved by 12.5% SDS-PAGE as described in Florea *et al.*[18] Wet gels were visualized using BioRad ChemiDoc imaging systems (BioRad, CA, USA; (λ_{ex} = 530 nm, λ_{em} = 560 nm). Fluorescence was normalized to a Coomassie Blue stained gel.

Cell-based activity-based probe activity

For cell-based analysis, ABP incubation was carried out as described in the preceding section. The working concentration was determined by serial dilutions and clearance of the fluorescence by Epox pre-incubation. Cultures were then washed with PBS (3×), 50 mM EDTA (1×) and methanol:PBS (1:1) (1×), and counterstained with Hoechst 33258 (Sigma Aldrich) (10 ng/mL). For imaging with Leica DM5500 fluorescent microscope, cells were seeded on glass, and after washing and dehydration cells were mounted with Citifluor (Le, UK). Images were taken using LAS AF software, version 2.3.6. High-throughput imaging was carried out with ArrayScan VTI HCA, Cellomics (Thermo Scientific), in cells seeds in a 96-well plate, images were taken directly after washings. Image analysis was carried out with the Cellomics

(Thermofisher) compartmental bio-application as described in Riaz *et al.*[14] In brief, the nucleus was defined as a reference, as detected by Hoechst staining. A 15 pixels ring from the segmented nucleus was defined for each cell, and LWA300 MFI was measured from both the nuclear part and the ring was referred all the cell MFI; the nuclear MFI was measured from the nuclear segmented circle. The same protocol was used to measure LWA300 in all conditions. Mean fluorescence is normalized to the area and to cultures incubated with LWA300 only.

For analysis with the flow cytometry, labelled cells were washed with PBS and were harvested by typsinization. Cells were collected in ice-cold PBS and were maintained on ice prior to analysis. ABP fluorescence was analysed using the BD-LSR II flow cytometer. Events were gated on size using the forward and side scatters (FSC and SSC; total 15 000 events), and subsequently, Hoechst positive events were included for the ABP MFI measurements. Analysis of fluorescence intensity was carried out with BD FACSDiva™ software version 8.0.1. MFI distribution curves were generated using FlowJo software suite version 7.6.5 (FlowJo, OR, USA). Background levels were determined by incubation with the unconjugated fluorophores: Bodipy-FL (LWA300, LW124, and PR592) and Bodipy-TMR (MV151, MVB003, and MVB127) (Thermofisher).

Mice and histological staining and fibre typing of muscle sections

Male, 5-week-old C57BL/6J mice (Jackson laboratories, Sacramento, CA, USA) were acclimatized for 1 week and standard conditions as detailed in Riaz *et al.*,[25] under the Animal Research: Reporting of In Vivo Experiments guidelines. An animal research protocol [#13113] was approved by the Institutional Animal Ethical Committee, Leiden University Medical Center, Leiden, the Netherlands. Muscles were harvested from 6-week-old mice. Cryosections (10 μm) were made using the CM3050S cryostat (Leica Microsystems). Muscle sections were pasted sequentially on super frost plus glass slides (Menzel-Gläser; Thermo scientific) and stored at −20 prior to staining. Prior to incubation with inhibitors, tissue was equilibrated with PBS/Tween 0.05%. Staining with LWA300 (0.05 μM) was carried out in PBS for 40 min. Pre-incubation was carried out with Epox 0.5 μM, NC-005 (0.5 μM), or DMSO (mock) in PBS for 1 h. Subsequently, sections were washed with PBS (3×), 50 mM EDTA (1×), and methanol:PBS (1:1) (1×), dehydrated with ethanol and mounted in Citifluor (Le, UK). All incubations were carried out at room temperature.

Myofiber typing was carried out in consecutive cryosections using antibodies to three myosin heavy chain isoforms conjugated as follows: type-2b with Alexa-488 (green), type-2a with Alexa-594 (red), and type-1 with

Alexa-350 (blue).[26] The immunofluorescence procedure was carried out as detailed in Riaz *et al.*[14,25] Images were captured with the DM5500 microscope (Leica) using the LAS AF software version 2.3.6. Image quantification in muscles was carried out with ImageJ https://imagej.nih.gov/ij/.

Statistical analyses

Unless otherwise indicated, statistical analyses were performed in Prism 7 (GraphPad software) and an unpaired *t*-test. Density plots were made in R-studio with the ggplot2 package.

Results and Discussion

Screening of six ABPs was carried out in C2C12 immortalized mouse myoblasts: three pan-reactive ABPs (LWA300,

MVB003, and MV151) and three subunit-specific probes (Figure 1A). LWA300 and MVB003 contain the natural compound Epoxomicin (Epox) core conjugated to BodipyFL or Bodipy TMR fluorophore, respectively.[18,27] MV151 is the product of chemical design with an $(Ahx)_3$ Leu_3 core attached at the C terminus to vinylsulphone electrophilic trap and at the N terminus to BodipyTMR.[17] LW124 contains a β1c/1i selective sequence with epoxyketone electrophilic trap and bodipy FL tag.[27] PR592 and MVB127 are β5c/5i directed probes with BodipyFL/epoxyketone and BodipyTMR/vinylsulphone fluorophore/reactive group pair, respectively.[20,21] Specific binding to an active proteasome was determined by pre-incubation with the proteasome inhibitor, Epox. Epox competes with ABP binding to the active proteasome subunits. ABP binding to active subunits was determined using activity gels (Figure 2). All three pan-reactive probes showed specific binding to the β2 and β5 subunits as Epox cleared the fluorescence signal (Figure 2A–2C). MVB003 binding to β1 was not specific (Figure 2B).

Figure 2 Screening for specific activity-based probes binding in muscle cell culture using activity gels. (A–C) Pan-reactive probes. (D–F) Subunit-specific activity-based probes. For each activity, probe representative gel images and Coomassie Blue stained gel are shown at the left side. A chart bar on the right side shows the band intensity for each subunit after normalization to Coomassie Blue loading control. Averages and standard variation are from three biological replicates. Grey bars show mock (DMSO pre-incubation followed by probe incubation) and black bars show pre-incubation with Epoxomicin followed by incubation with the proteasome activity probe. Average and standard deviations are from three independent cultures, statistical significance ($p < 0.05$; *) was assessed by the Student's *t*-test.
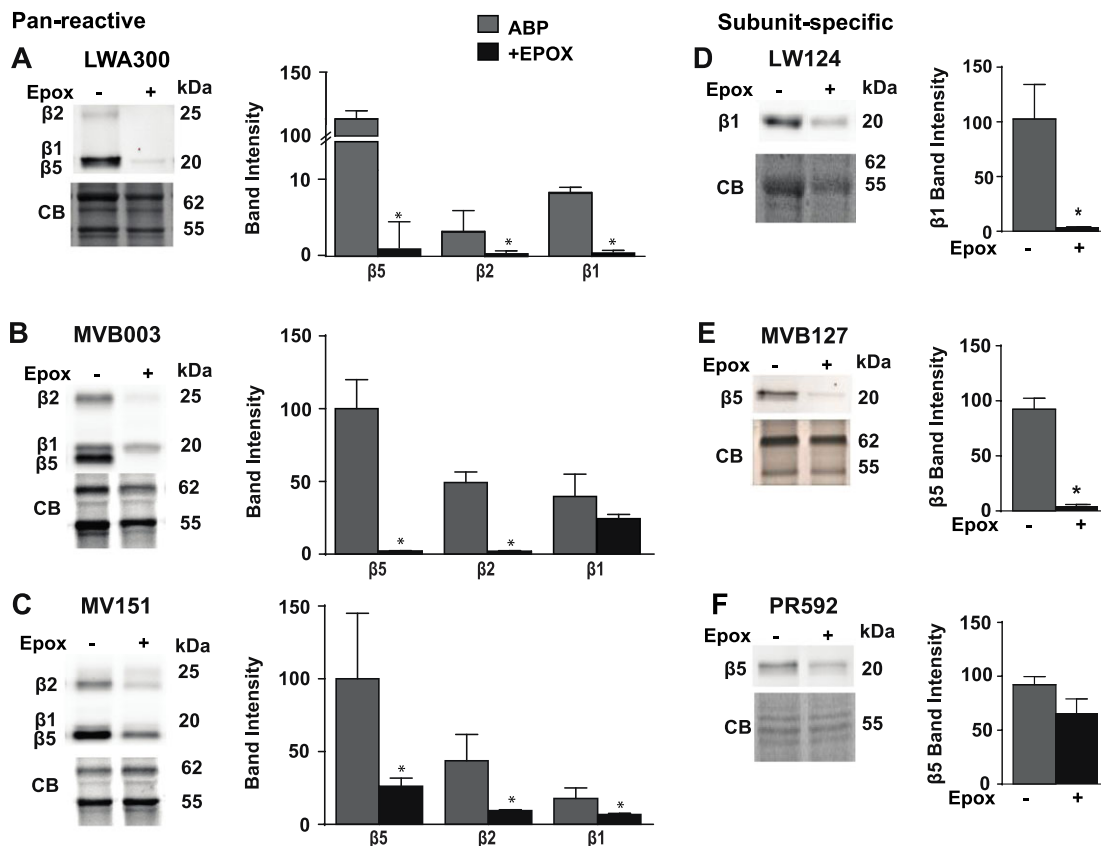
Binding of MV151 was the least specific (Figure 2C), possibly because it is a first-generation probe and is more hydrophobic.[17] Amongst the pan-reactive ABPs, LWA300 showed the most specific binding (Figure 2A). Of the subunit-specific ABPs, binding of LW124 to the β1 subunit and that of MVB127 to the β5 subunit was found to be specific in C2C12 myoblasts (Figure 2D–2E). However, PR592 displayed no decrease in fluorescence following pre-incubation in Epox, indicating lack of specificity (Figure 2F). With all three pan-reactive probes, the signal from β5 was higher compared with β1 and β2 in the muscle cell culture (Figure 2A–2C).

Specific binding in C2C12 cell culture was further assessed by pre-incubation with the MG132, and reduced LWA300 signal fluorescence was found for β5, β1, and β2 subunits (Figure 3A). However, MG132 competition with LWA300 binding to β5 and β2 was less effective compared with Epox. This observation is in agreement with recent studies showing that MG132 inhibition of proteasome activity is less specific

than Epox.[28] In addition, pre-incubation with NC-005, an inhibitor of β5 subunit, led to a reduction in the β5 signal whilst fluorescence in β2 and β1 is unaffected (Figure 3B).

To assess whether altered proteasome activity, we generated stable Usp14-knockdown in C2C12 using shRNA to Usp14 (Figure 3C and 3D). Compared with scramble (scram) cell culture, β5 and β1 signals in shUsp14 were significantly increased, whereas β2 signal less unaffected (Figure 3E). Moreover, β5 and β1 signals were also elevated in scram cell culture after pre-incubation with IU1, an Usp14 inhibitor (Figure 3E). Inhibition of Usp14 elevates proteasome activity in mouse fibroblasts cell culture.[29] Our study suggests that Usp14 predominantly affects β5 activity in C2C12 cell culture.

The pattern of signal from the β-subunits in C2C12 cells differ from that reported in HeLa cells. In HeLa cells, all three β-subunits show similar signal intensity,[17] but in the muscle cell culture, we found that the β5 signal is two-fold to four-fold higher than β2 and β1, respectively. We recently

Figure 3 Verification of LWA300 specific activity in C2C12 cell culture. (A) MG132 (10 mM) pre-incubation competes with LWA300 binding to β-subunits. The image shows a representative activity gel, and the bar chart shows signal quantification. (B) NC-005 (1 μM) pre-incubation competes with LWA300 binding to the β5-subunit. The image shows a representative activity gel, and the bar chart shows signal quantification. (C–D) Usp14 stable KD in C2C12. (C) Usp14 levels were measured using RT-qPCR; fold change was calculated after normalization to Hprt and scramble control. Average and standard deviation are from three biological replicates. (D) Western blot shows Ups14 protein levels. Tubulin shows equal loading. (E) LWA300 binding to β-subunits in shUps14 and IU1-treated scramble cells. The image shows a representative activity gel and the corresponding Coomassie Blue staining and bar chart shows signal quantification. For all activity gels, the band intensity for each subunit is normalized to Coomassie Blue loading control. Averages and standard variation are from three biological replicates. Statistical significance ($p < 0.05$; *) was assessed by the Student's *t*-test.
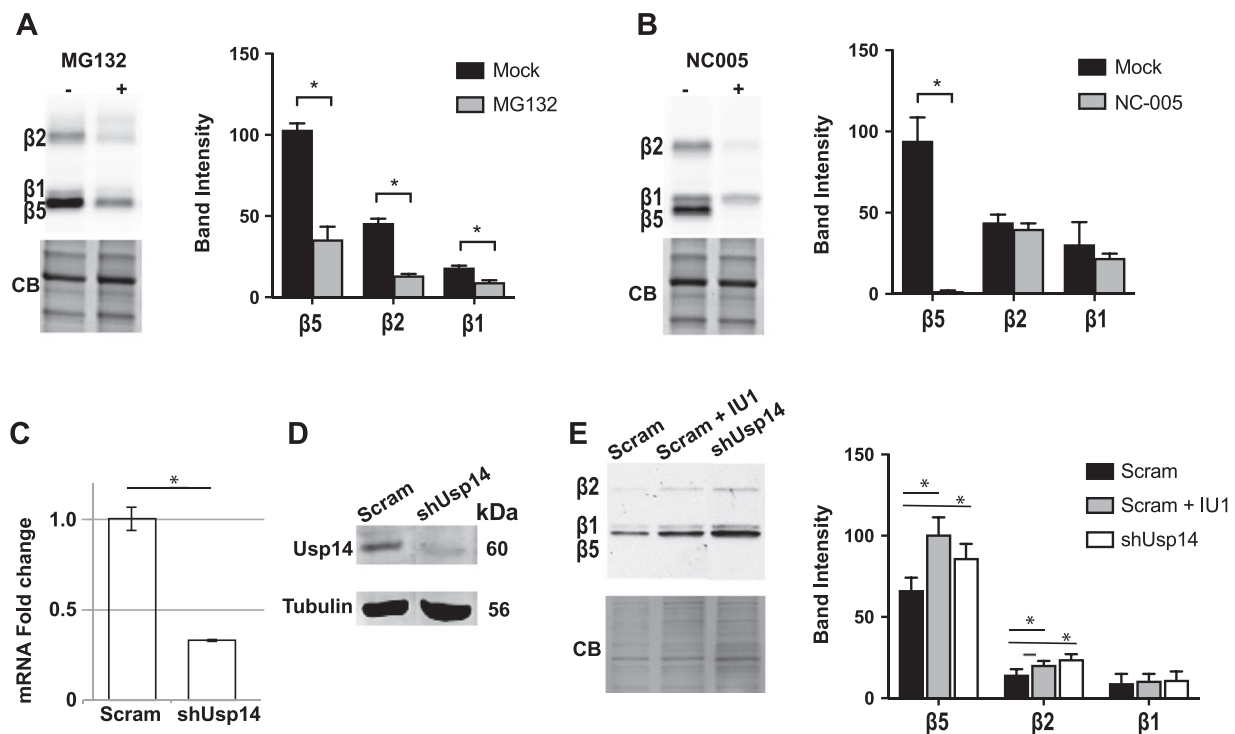
reported that in the C2C12 cell culture, β5 protein levels are lower than β2;[14] this indicates that β5 activity in C2C12 is higher than β2 activity. Also, in mouse thymus, the β5 signal is higher compared with the other subunits.[18] Thus, specific proteasomal activity in cells and tissues should include subunit-specific analysis.

The probes with most specific binding (LWA300, LW124, and MVB127) were then applied in cell-based imaging assays. For high-throughput imaging, we tested specificity in cells using flow cytometry. Signal specificity was determined by pre-incubation with Epox, and Hoechst was used to gate the living cells (Figure 4A). A concentration curve reveals differences in signal specificity between the ABPs (Figure 4B). The LWA300 signal was found to be the most specific as fluorescence was abolished by Epox pre-incubation (Figure 4B). LW124 and MVB127 staining was found to be less or not specific, respectively (Figure 4B). Imaging of the

ABPs signal in adherent C2C12 cells confirmed that the MVB127 signal in cells was not reduced in Epox-treated cells (Figure 4C). The MVB127 non-specific signal was mostly localized to membrane structures because of its lipophilic property.[18] The LW124 non-specific signal was found in the nucleus (Figure 4C). LWA300 fluorescence was found in both nuclear and cytoplasmic compartments, and Epox pre-incubation abolished the fluorescence signal from both compartments (Figure 4C). Together, those experiments indicate that ABPs are suitable to monitor proteasome activity in intact cells using flow cytometry.

Flow cytometry in muscle cell culture possesses a number of shortcomings, as differentiated multinucleated muscle cells are too large for the conventional flow cytometry. We then assessed LWA300 fluorescence in adherent and fused C2C12 cell cultures using the Cellomics imaging system. In previous studies, we demonstrated that this imaging system

Figure 4 Cell-based quantification of proteasomal activity in C2C12 immortalized murine cell culture. (A–B) Analysis of activity-based probes specific binding in living C2C12 cells using flow cytometry. (A) Distribution plots show LWA300 (green) and Hoechst (blue) mean fluorescence intensity in mock (LWA300) and Epoxomicin-treated cell cultures. (B) Plots show a concentration curve of the average mean fluorescence intensity for LWA300, LW124, or MVB127 in mock or Epoxomicin-treated cell cultures. Average mean fluorescence intensity was calculated from ~10 000 cells per treatment. Averages and standard variations are from three replicates. (C) Images show activity-based probe fluorescence distribution within C2C12 cells: LWA300 (green), LW124 (green), or MVB127 (red) in mock or pre-incubation with Epoxomicin. The cell nucleus is stained with DAPI. In the upper right box in each image, a single nucleus without a DAPI overlap is shown, and the same nucleus is marked with a yellow ring in the overlay image. Scale bar 7.5 μm. (D) Images of LWA300 signal in C2C12 cells. The right panel shows cells after pre-incubation with Epoxomicin. Colour images show overlay between LWA300 and Hoechst. A grey-scale image of LWA300 signal is shown in the upper right box, and nuclear segmentation by the Cellomics software is depicted with a circle. (E) Bar chart shows LWA300 mean fluorescence intensity measurements in flow cytometry and Cellomics, in mock or pre-treatment with Epoxomicin, NC-005 or NC-001. Measurements in Cellomics were carried out for the nuclear (N) fraction or the preinuclear + nuclear regions (P + N). Means and standard deviations are depicted. Measurements were normalized to mock-treated cells. Averages and standard deviations are from three biological replicates; in each condition, flow cytometry averages are from ~10 000 cells, and Cellomics averages are from ~3000 cells.
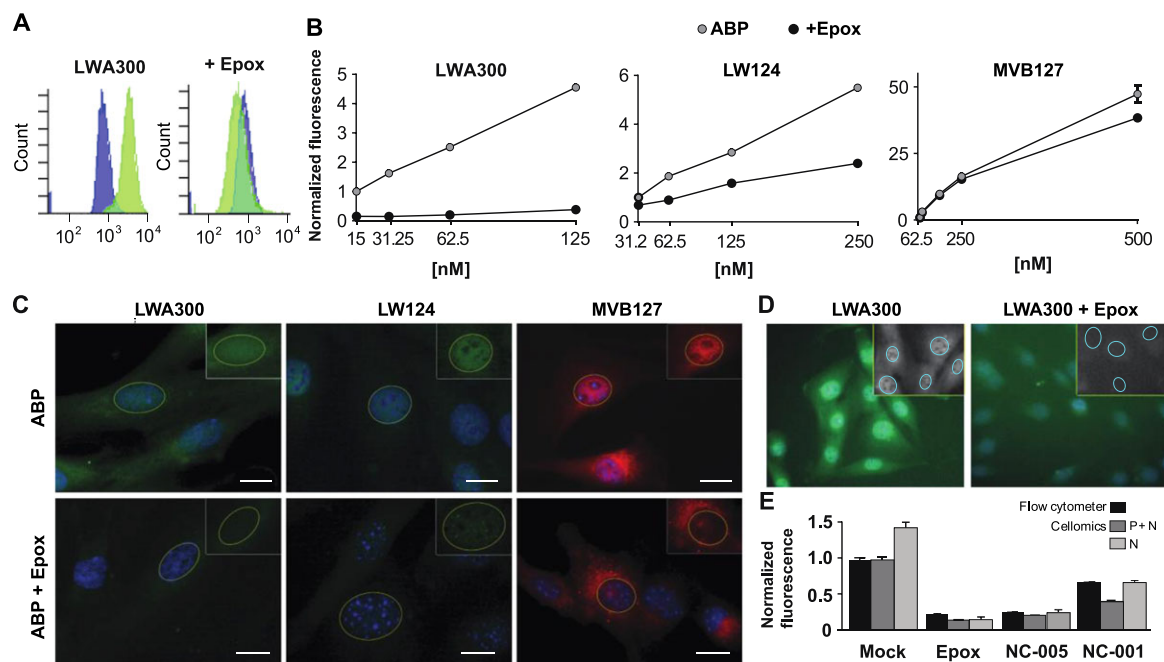
is highly suitable for high-throughput of fused muscle cell cultures.[24,30] In agreement with the flow cytometry experiments, also with the Cellomics, we measured the reduced LWA300 signal by Epox pre-incubation (Figure 4D–4E). Using the Cellomics tools, we assessed the LWA300 signal in the nucleus, and found an enrichment of nuclear signal in C2C12 cells (Figure 3E). We then also investigated subunit-specific activity in the C2C12 muscle cell culture using pre-incubation with the NC-005 or NC-001 β5 or β1 specific inhibitors, respectively. Consistently, NC-005 was found to be more effective compared with NC-001 (Figure 4E). This suggests that β5 is more active in C2C12 cells moreover in the cell nucleus. This conclusion is also consistent with the higher β5 activity that was observed by activity gels.

The immortalized human muscle cells (7304.1) exhibit a high fusion index and are more suitable for analyses of fused cells as compared with C2C12 cells.[30] We compared proteasomal activity in fused cultures and found a higher LWA300 signal in fused human muscle cells compared with non-fused cultures (Figure 5A). Confirming the results in the mouse C2C12 myoblasts, LWA300 binding was competed with Epox or NC-005 pre-treatment, whereas pre-treatment with NC-001 had little effect on the LWA300 signal (Figure 5B). In fused cells, the LWA300 average signal in the cell nucleus was nearly three-fold higher compared with non-fused cultures, and the average signal in the perinuclear cytoplasmic region was 1.5-fold higher (Figure 5C). This indicates that proteasomal activity in muscle cells varied between cell compartments and changes within cell compartments could alter during cell fusion. Enrichment of proteasomal subunits in the nuclear fraction was previously reported in rat liver and several non-muscle cells.[31] Dynamic sub-cellular distribution of proteasomal subunits was found in cancer cell cultures, and components of the 19S were enriched in the nuclear fraction.[32] The change in proteasomal activity during cell fusion could also be due to the increase in expression of specific subunits. Nevertheless, these results reveal that proteasomal activity increases in fused cultures.

Figure 5 Cell-based quantification of proteasomal activity in 7304.1 immortalized human myoblasts. (A) Representative images of the LWA300 signal in non-fused or fused cell cultures. The colour image shows the overlay between LWA300 and Hoechst. The grey-scale images show LWA300 signal. The nuclear region is within the cyan circle, and the peri-nuclear region is situated between the nuclear circle and the yellow ring. The scale bar is 20 μm. (B) The bar chart shows LWA300 mean fluorescence intensity normalized to mock-treated in Epoxomicin, NC-001, and NC-005 treated cell cultures. Averages and standard deviations are from three replicates. (C) The bar chart shows LWA300 mean fluorescence intensity in non-fused and fused 7304.1 cell cultures in the nuclear and perinuclear regions. Shown are mean fluorescence intensity and standard error. Significant difference ($p < 0.05$) between mock and treatment was assessed by the student's *t*-test and is denoted with *.
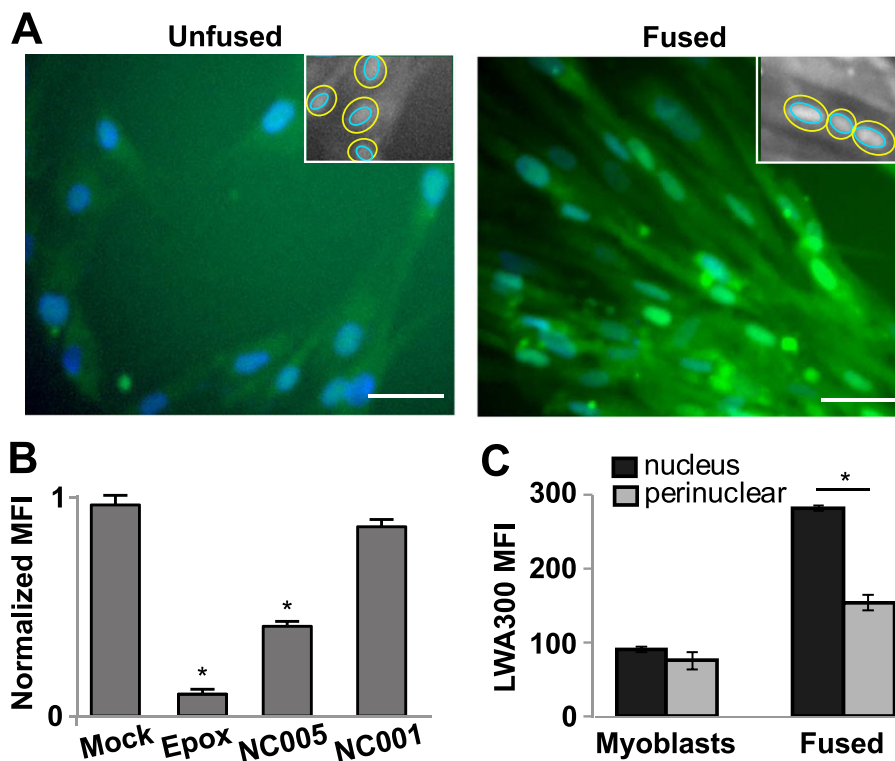
We then examined LWA300-specific binding in mouse quadriceps muscle cryosections. The LWA300 signal in myofibers was abolished by pre-incubation with Epox or NC-005, and tissue auto-fluorescence was not detectable by the imaging conditions that were used to image the LWA300 signal (Figure 6Aa–d). At a higher magnification, the LWA300 signal form puncta were visible in both cross sections and longitudinal sections (Figure 6Ae–f). Those puncta could represent active proteasomes in the endoplasmatic reticulum, as the proteasome is enriched in the endoplasmatic reticulum in muscles.[33] As expected, the LWA300 signal was also found within myonuclei, as determined by the overlap with DAPI staining (Figure 6Ae). Most striking, the LWA300 signal varied between myofibers (Figure 6Ab).

To assess whether proteasome activity differs between muscles, LWA300 staining was performed in two fast-twitch muscles (quadriceps and gastrocnemius), and in soleus and slow-twitch muscle (Figure 6B). Mean fluorescence intensity (MFI) was measured within each myofiber, and differences in MFI were assessed using density plots (Figure 6C), revealing a distinguished pattern for each muscle. Most noticeable, the fast-twitch muscles showed higher LWA300 fluorescence compared with the slow-twitch muscle (Figure 6C). In addition, the MFI distribution was narrow in

Figure 6 Proteasomal activity in myofibers of mouse muscles. (A) LWA300 binding specificity in quadriceps muscle cryosections. (a) A negative control shows auto fluorescence. (b–f) incubation with LWA300 (b, e–f) or pre-incubated with Epox (c) or NC-005 (d). The scale bars are 50 um (a–d), 10 um (e), 25 um (f). (a–e) show cross-sections and (f) shows longitudinal section. (e) In the upper box, LWA300 co-localization with DAPI is shown. (B) LWA300 staining (upper row) in myofiber types (lower row) in quadriceps, soleus and gastrocnemius muscles. Myofiber typing was carried out using immunohistochemistry to MyHC-2b (green), MyHC-2a (red), or MyHC-1 (blue). Examples of corresponding myofibers between the sequential images are designated with numbers. The scale bar is 50 μm. (C) Density plots show LWA300 mean fluorescence intensity distribution across myofibers. Per muscle, over 150 myofibers are included. (D) Distribution plots show per myofibers mean fluorescence intensity of LWA300 and the three myosin heavy chain isotypes in each muscle. LWA300 mean fluorescence intensity sorts myofibers. Myofiber type profile is depicted. Hybrid myofiber indicates the expression of at least two mean fluorescence intensity isotypes.
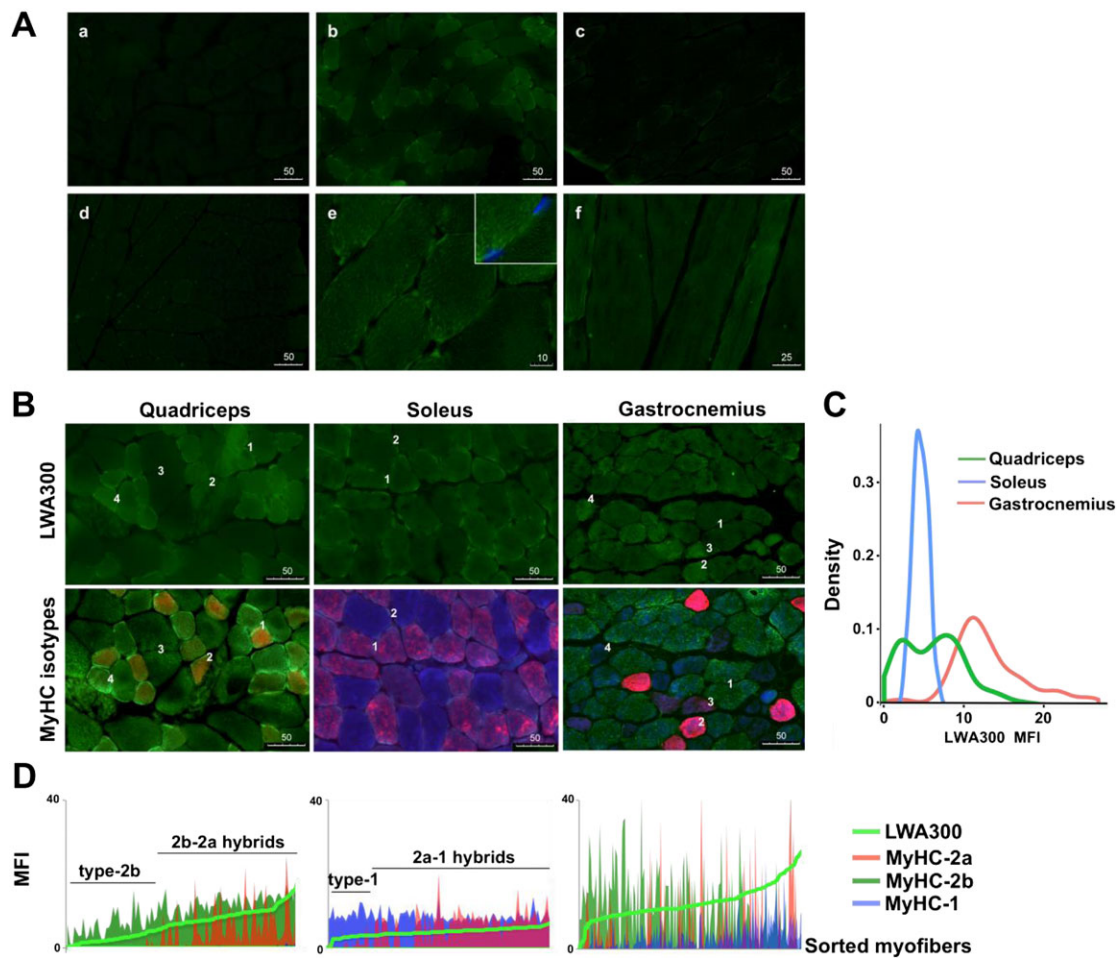
soleus—suggesting homogeneous staining across myofiber types, whereas in quadriceps and gastrocnemius, MFI distribution was broad, suggesting heterogeneity in proteasomal activity between myofibers. We then investigated whether LWA300 correlates with a myofiber type. A muscle is composed of different myofibers that can be distinguished by the expression of myosin heavy chain (MyHC) isotypes.[34] We assessed whether LWA300 intensity is associated with myofiber type in sequential cryosections that were stained for LWA300 or with a mix of conjugated antibodies to MyHC type-2b, type-2a, and type-1. Fluorescence intensity of LWA300 and MyHC isotypes was quantified per myofiber, and an association between LWA300 MFI and myofiber type was assessed in three muscles. In quadriceps, higher LWA300 MFI was predominantly found in hybrids expressing MyHC-2b and -2a, (Figure 6D; Quadriceps), whereas myofibers with a dominant MyHC-2b had a lower LWA300 signal (Figure 5D; Quadriceps). In soleus muscle, MyHC-2a and MyHC-1 are predominantly expressed whilst MyHC-2b is scarce. A higher LWA300 signal was found in hybrid myofibers expressing MyHC-1 and 2a (Figure 6D; Soleus). In myofibers with a dominant MyHC-1 staining, LWA300 signal was lower (Figure 6D; Soleus). Thus, the higher LWA300 signal was found in hybrid myofibers in both quadriceps and soleus. We then also investigated the LWA300 signal within myofibers in the gastrocnemius muscle, in which all three MyHC isotypes are co-expressed.[35] Overall, LWA300 was higher in gastrocnemius compared with soleus or quadriceps, and most myofibers expressed at least two MyHC isotypes. A lower LWA300 signal was found in myofibers expressing MyHC-2b (Figure 6D; Gastrocnemius), whereas a higher LWA300 signal was found in hybrid myofibers expressing MyHC-1 and -2a, or 2b-2a (Figure 5D; Gastrocnemius). Higher proteasomal activity in hybrid myofibers, irrespective of oxidative or glycolytic state, suggests that hybrid fibres require a higher protein turnover. The biological impact of hybrid myofibers could represent a transition phase between oxidative or glycolytic state.[14] The biological impact of hybrid myofibers is not fully understood, and an increase in hybrid myofibers was found during muscle repair.[36] Together, our study reveals that proteasomal activity differ between myofibers and between muscles.

Skeletal muscle function in the mammalian body is highly diverse with respect to fatigue resistance and response time of the twitch, reflected by a dynamic pattern of histochemical properties.[26] Our studies revealed a muscle-specific pattern of LWA300 staining. The heterogeneity of myofiber types, as determined by MyHC isotype expression, reflects primarily an adaptation to the different temporal and spatial activities of skeletal muscles.[26] Here, we show that proteasomal activity differ between myofibers, suggesting that proteasomal activity contributes to changes in myofiber function and

adaptation to prevailing conditions. Protein homeostasis and the ubiquitin proteasome system play a central role in muscle atrophy.[37,38] In a recent study, we found that the LWA300 signal is reduced within myofibers of the tibialis anterior muscle in a model for muscle ageing; specifically, the reduced LWA300 signal was found in atrophic myofibers.[14] This suggests that measuring proteasomal activity in muscles in different conditions could contribute to understand the pattern of myofiber function in different muscles.

In conclusion, this study demonstrated that the pan-reactive LWA300 is the most consistently specific probe for the detection of proteasomal activity in muscle cells and tissue. We show that proteasomal activity differs between myofibers, and under normal conditions, a higher proteasomal activity was found in hybrid myofiber expressing MyHC-2a, whereas myofibers that predominantly express one MyHC isotype showed a low LWA300 signal. As proteasomal activity plays a central role in neuromuscular disorders and aged muscles, and the ubiquitin–proteasome system plays a prominent role in muscle protein homeostasis, we suggest that measuring proteasomal activity could be valuable to understand changes in muscle pathology. The application of ABPs in cancer cells demonstrated to accurately measure protein homeostasis and its restoration response to drugs.[39,40] Future studies could explore the application of ABPs to monitor progression in muscle pathology and treatment efficacy in muscular dystrophies.

Acknowledgements

Authors' contribution

V.R. conceived and designed the experiments. C.R., C.O., Y.R., M.R., and G.P.S. performed the experiments. Y.R. and V.R. analysed the data. B.I.F. contributed reagents/materials/analysis tools. V.R., B.I.F., and Y.R. wrote the MS.

Conflict of interest

None declared.

References

1. Martens S, Bachmair A. How cells coordinate waste removal through their major proteolytic pathways. *Nat Cell Biol* 2015;**17**:841–842.

2. Sandri M, Coletto L, Grumati P, Bonaldo P. Misregulation of autophagy and protein degradation systems in myopathies and muscular dystrophies. *J Cell Sci* 2013;**126**:5325–5333.

3. Lilienbaum A. Relationship between the proteasomal system and autophagy. *Int J Biochem Mol Biol* 2013;**4**:1–26.

4. Cardinale A, Chiesa R, Sierks M. Protein Misfolding and Neurodegenerative Diseases. *Int J Cell Biol* 2014;**2014**:217371.

5. Bedford L, Paine S, Sheppard PW, Mayer RJ, Roelofs J. Assembly, structure, and function of the 26S proteasome. *Trends Cell Biol* 2010;**20**:391–401.

6. Groll M, Heinemeyer W, Jager S, Ullrich T, Bochtler M, Wolf DH, et al. The catalytic sites of 20S proteasomes and their role in subunit maturation: a mutational and crystallographic study. *Proc Natl Acad Sci U S A* 1999;**96**:10976–10983.

7. Carmony KC, Kim KB. Activity-Based Imaging Probes of the Proteasome. *Cell Biochem Biophys* 2013;**67**:91–101.

8. Sieber SA. *Activity-Based Protein Profiling*. Springer Heidelberg Dordrecht. New York: Springer Science & Business Media; 2012.

9. Kisselev AF, Groettrup M. Subunit specific inhibitors of proteasomes and their potential for immunomodulation. *Curr Opin Chem Biol* 2014;**23**:16–22.

10. Liggett A, Crawford LJ, Walker B, Morris TC, Irvine AE. Methods for measuring proteasome activity: current limitations and future developments. *Leuk Res* 2010;**34**:1403–1409.

11. Lecker SH, Goldberg AL, Mitch WE. Protein degradation by the ubiquitin-proteasome pathway in normal and disease states. *J Am Soc Nephrol* 2006;**17**:1807–1819.

12. Ferrington DA, Husom AD, Thompson LV. Altered proteasome structure, function, and oxidation in aged muscle. *FASEB J* 2005;**19**:644–646.

13. Altun M, Besche HC, Overkleeft HS, Piccirillo R, Edelmann MJ, Kessler BM, et al. Muscle wasting in aged, sarcopenic rats is associated with enhanced activity of the ubiquitin proteasome pathway. *J Biol Chem* 2010;**285**:39597–39608.

14. Riaz M, Raz Y, van Putten M, Paniagua-Soriano G, Krom YD, Florea BI, et al. PABPN1-Dependent mRNA Processing Induces Muscle Wasting. *PLoS Genet* 2016;**12**:e1006031.

15. Hepple RT, Qin M, Nakamoto H, Goto S. Caloric restriction optimizes the proteasome pathway with aging in rat plantaris muscle: implications for sarcopenia. *Am J Physiol Regul Integr Comp Physiol* 2008;**295**:R1231–R1237.

16. Trollet C, Anvar SY, Venema A, Hargreaves IP, Foster K, Vignaud A, et al. Molecular and phenotypic characterization of a mouse model of oculopharyngeal muscular dystrophy reveals severe muscular atrophy restricted to fast glycolytic fibres. *Hum Mol Genet* 2010;**19**:2191–2207.

17. Verdoes M, Florea BI, Menendez-Benito V, Maynard CJ, Witte MD, van der Linden WA, et al. A fluorescent broad-spectrum proteasome inhibitor for labeling proteasomes in vitro and in vivo. *Chem Biol* 2006;**13**:1217–1226.

18. Florea BI, Verdoes M, Li N, van der Linden WA, Geurink PP, van den Elst H, et al. Activity-based profiling reveals reactivity of the murine thymoproteasome-specific subunit beta5t. *Chem Biol* 2010;**17**:795–801.

19. Li N, Kuo CL, Paniagua G, van den Elst H, Verdoes M, Willems LI, et al. Relative quantification of proteasome activity by activity-based protein profiling and LC-MS/MS. *Nat Protoc* 2013;**8**:1155–1168.

20. Verdoes M, Willems LI, van der Linden WA, Duivenvoorden BA, van der Marel GA, Florea BI, et al. A panel of subunit-selective activity-based proteasome probes. *Org Biomol Chem* 2010;**8**:2719–2727.

21. Geurink PP, Florea BI, Li N, Witte MD, Verasdonck J, Kuo CL, et al. A cleavable linker based on the levulinoyl ester for activity-based protein profiling. *Angew Chem Int Ed Engl* 2010;**49**:6802–6805.

22. Britton M, Lucas MM, Downey SL, Screen M, Pletnev AA, Verdoes M, et al. Selective inhibitor of proteasome's caspase-like sites sensitizes cells to specific inhibition of chymotrypsin-like sites. *Chem Biol* 2009;**16**:1278–1289.

23. de Klerk E, Venema A, Anvar SY, Goeman JJ, Hu O, Trollet C, et al. Poly(A) binding protein nuclear 1 levels affect alternative polyadenylation. *Nucleic Acids Res* 2012;**40**:9089–9101.

24. Anvar SY, Raz Y, Verway N, van der Sluijs B, Venema A, Goeman JJ, et al. A decline in PABPN1 induces progressive muscle weakness in oculopharyngeal muscle dystrophy and in muscle aging. *Aging (Albany NY)* 2013;**5**:412–426.

25. Riaz M, Raz Y, Moloney EB, van Putten M, Krom YD, van der Maarel SM, et al. Differential myofiber-type transduction preference of adeno-associated virus serotypes 6 and 9. *Skelet Muscle* 2015;**5**:37.

26. Schiaffino S, Reggiani C. Fiber types in mammalian skeletal muscles. *Physiol Rev* 2011;**91**:1447–1531.

27. Willems LI, van der Linden WA, Li N, Li KY, Liu N, Hoogendoorn S, et al. Bioorthogonal chemistry: applications in activity-based protein profiling. *Acc Chem Res* 2011;**44**:718–729.

28. Kreidenweiss A, Kremsner PG, Mordmuller B. Comprehensive study of proteasome inhibitors against Plasmodium falciparum laboratory strains and field isolates from Gabon. *Malar J* 2008;**7**:187.

29. Lee B-H, Lee MJ, Park S, Oh D-C, Elsasser S, Chen P-C, et al. Enhancement of proteasome activity by a small-molecule inhibitor of USP14. *Nature* 2010;**467**:179–184, supplementary-information.

30. Raz V, Buijze H, Raz Y, Verwey N, Anvar SY, Aartsma-Rus A, et al. A novel feed-forward loop between ARIH2 E3-ligase and PABPN1 regulates aging-associated muscle degeneration. *Am J Pathol* 2014;**184**:1119–1131.

31. Brooks P, Fuertes G, Murray RZ, Bose S, Knecht E, Rechsteiner MC, et al. Subcellular localization of proteasomes and their regulatory complexes in mammalian cells. *Biochem J* 2000;**346**:155–161.

32. Fabre B, Lambour T, Delobel J, Amalric F, Monsarrat B, Burlet-Schiltz O, et al. Subcellular Distribution and Dynamics of Active Proteasome Complexes Unraveled by a Workflow Combining in Vivo Complex Cross-Linking and Quantitative Proteomics. *Mol Cell Proteomics* 2013;**12**:687–699.

33. Wojcik C, DeMartino GN. Intracellular localization of proteasomes. *Int J Biochem Cell Biol* 2003;**35**:579–589.

34. LaFramboise WA, Daood MJ, Guthrie RD, Schiaffino S, Moretti P, Brozanski B, et al. Emergence of the mature myosin phenotype in the rat diaphragm muscle. *Dev Biol* 1991;**144**:1–15.

35. Hayasaki H, Shimada M, Kanbara K, Watanabe M. Regional difference in muscle fiber type and glucose uptake of mouse gastrocnemius at rest. *Cell Mol Biol (Noisy-le-Grand)* 2001;**47**: OL135–OL140.

36. Matsuura T, Li Y, Giacobino JP, Fu FH, Huard J. Skeletal muscle fiber type conversion during the repair of mouse soleus: potential implications for muscle healing after injury. *Journal of orthopaedic research : official publication of the Orthopaedic Research Society* 2007;**25**:1534–1540.

37. Bonaldo P, Sandri M. Cellular and molecular mechanisms of muscle atrophy. Disease Models &amp. *Mechanisms* 2013;**6**:25–39.

38. Mitch WE, Goldberg AL. Mechanisms of Muscle Wasting — The Role of the Ubiquitin–Proteasome Pathway. *N Engl J Med* 1996;**335**:1897–1905.

39. Nomura DK, Dix MM, Cravatt BF. Activity-based protein profiling for biochemical pathway discovery in cancer. *Nat Rev Cancer* 2010;**10**:630–638.

40. Bassermann F, Eichner R, Pagano M. The ubiquitin proteasome system - implications for cell cycle control and the targeted treatment of cancer. *Biochim Biophys Acta* 2014;**1843**:150–162.

41. von Haehling S, Morley JE, Coats AJS, Anker SD. Ethical guidelines for publishing in the Journal of Cachexia, Sarcopenia and Muscle: update 2015. *J Cachexia Sarcopenia Muscle* 2015;**6**:315–316.